UC Davis

UC Davis Previously Published Works

Title

Insight into pH dependent Cr(VI) removal with magnetic Fe3S4

Permalink

https://escholarship.org/uc/item/1sk3784g

Authors

Liu, Wei
Jin, Lide
Xu, Jin
et al.

Publication Date

2019-03-01

DOI

10.1016/j.cej.2018.11.192

Peer reviewed

eScholarship.org Powered by the California Digital Library
University of California

Chemical Engineering Journal 359 (2019) 564–571

Contents lists available at ScienceDirect

Chemical Engineering Journal

journal homepage: www.elsevier.com/locate/cej

Insight into pH dependent Cr(VI) removal with magnetic Fe_3S_4

Wei Liu[a], Lide Jin[a], Jin Xu[a], Jia Liu[a], Yanyan Li[a], Peipei Zhou[a], Cuicui Wang[a], Randy A. Dahlgren[a,b], Xuedong Wang[a,*]

[a] Zhejiang Provincial Key Laboratory of Watershed Science and Health, Southern Zhejiang Water Research Institute, Wenzhou Medical University, Wenzhou 325035, People's Republic of China

[b] Department of Land, Air and Water Resources, University of California, Davis, CA 95616, United States

HIGHLIGHTS

- Magnetic Fe_3S_4 was used to remove Cr (VI).
- Adsorption, reduction and precipitation were involved in Cr(VI) removal process.
- Cr(VI) removal mechanisms were extremely dependent on solution pH.
- Surface Fe(III)/Fe(II) cycles mediated by structural sulfides promoted Cr(VI) removal.

GRAPHICAL ABSTRACT

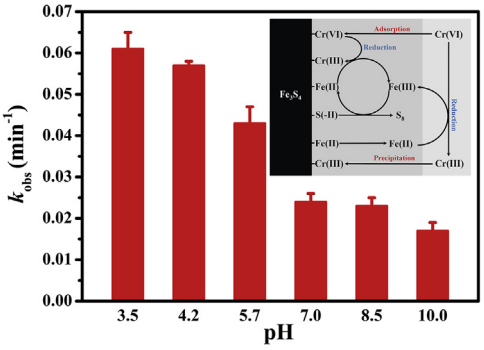

ARTICLE INFO

Keywords:
Greigite (Fe_3S_4)
Cr(VI)/Cr(III)
Adsorption
Reduction
Surface reaction

ABSTRACT

In this study, an magnetically separable iron sulfide (greigite, Fe_3S_4) was synthesized by solvothermal method and employed for effective removal of Cr(VI). The Cr(VI) removal process followed a pseudo-first-order kinetic model that was highly dependent on the initial Fe_3S_4:Cr(VI) molar ratio. The total Cr(VI) removal was involved in surface adsorption/reduction and solution reduction/precipitation processes via electrostatic attraction, electron transfer and co-precipitation mechanisms. The apparent Cr(VI) removal rate constants decreased from 0.061 to 0.017 min^{-1} with solution pH increased from 3.5 to 10.0, which resulted from the higher reducibility and surface electropositivity of Fe_3S_4 at low pH. The 1,10-phenanthrolin inhibitory experiment revealed that the Cr(VI) reduction process was mainly mediated by ferrous ions rather than sulfides. By means of analyses on the iron and sulfur species, the efficient Cr(VI) removal with Fe_3S_4 was ascribed to the surface Fe(III)/Fe(II) cycles induced by the sulfide ions. As for the reusability of Fe_3S_4, the Cr(VI) removal efficiency after 3 cycles was decreased to ca. 50% under the same conditions, which may be caused by the generation of Cr (oxide)hydroxyl and sulfide. These findings provide new insights into the concerned chromate transfer mechanisms mediated by magnetic iron sulfides, and have great prospects in construction of highly efficient systems for the Cr(VI) removal.

* Corresponding author.
E-mail address: wxdong@wzmc.edu.cn (X. Wang).

https://doi.org/10.1016/j.cej.2018.11.192
Received 6 September 2018; Received in revised form 23 November 2018; Accepted 24 November 2018
Available online 24 November 2018
1385-8947/ © 2018 Elsevier B.V. All rights reserved.

1. Introduction

Chromium (Cr) is widely used in industrial processes, such as textile dying, tanneries, galvanic industry and wood preservation [1,2]. Due to its dissolubility, persistence and bioaccumulation, Cr is frequently detected in groundwater, surface water and soil [3]. There are several oxidation states of Cr in the environment, and the most common and stable forms are Cr(III) and Cr(VI) species, which exhibits extremely contrasting properties [4]. For instance, Cr(VI) including $HCrO_4^-$ and $Cr_2O_7^{2-}$ are soluble, highly mobile in water and exert toxic effects on biological systems. In contrast, Cr(III) is much less toxic in natural aquatic environment duo to the formation of insoluble species, such as $Cr(OH)_3$ or $Cr_xFe_{1-x}(OH)_3$ [5,6]. Thus, Cr(VI) has been identified as a top priority hazardous pollutant by the United States Environmental Protection Agency (USEPA), and its mandatory discharge limit in China is regulated to be 0.05 and 0.5 mg/L in surface water and wastewater, respectively [7]. As a consequence, it is a great challenge to develop methods to efficiently remove Cr(VI) from the water environment.

The most common approach to remediate Cr(VI) pollution is to reduce Cr(VI) into relatively less bioavailable and toxic Cr(III) by chemical reduction methods [8]. For example, ferrous ions, sulfides, and organic compounds were widely used for the reduction of Cr(VI) attributing to their lower redox potential [9–12]. Seama et al. and Schlautman et al. demonstrated that dissolved ferrous ions could reduce Cr(VI) under neutral pH, and the Cr(VI) removal efficiencies were dependent on the solution pH value, the kinds of ligands and buffers, and the dissolved oxygen concentration [13,14]. Kim et al. found that the sulfide could efficient reduce Cr(VI) into Cr(III), and the reductive efficiency was strongly dependent on the ionic strength and solution pH [15]. Li et al. concluded that Fe(III) could promote the Cr(VI) reduction induced by sodium borohydride [16]. Unfortunately, these homogeneous reductive processes could not decrease the total Cr species in the solution, and need the following of precipitation with alkali, which may increase the cost of the treatment and cause the secondary pollution. Therefore, it is imperative to find an efficient, cost-effective and environmentally benign method to realize the Cr(VI) reduction and Cr (III) immobilization.

Iron materials, such as zero-valent iron (ZVI), iron (oxide)hydroxyl, and iron sulfides, are commonly used to reduce and/or adsorb the Cr (VI) [17–19]. For example, it was found that Cr(VI) reductive efficiency induced by ZVI was much higher than that of ferrous ions and sulfite, which may be caused by the multiple electron donators such as ZVI, the structure and dissolved ferrous ions [20]. Moreover, due to its excellent affinity of heavy metals, iron minerals can easily adsorb the generated Cr(III) species to realize the total Cr immobilization on its surface [21,22]. However, ZVI is easily oxidized at ambient conditions to form a oxidative layer on ZVI surface, which may block its further oxidation by Cr(VI) [23].

Due to simultaneous containing of Fe(II) and S(-II) species, iron sulfides are widely used as an efficient reductant for Cr(VI) remediation [24–28]. Patterson et al. found that the Cr(VI) in the soil and water environment was efficiently reduced by FeS to generate $[Cr_{0.75}Fe_{0.25}](OH)_3$ via a reduction-coprecipitation route [29]. More interestingly, the higher Cr(VI) reduction efficiency is induced by the structural ferrous ions and sulfide rather than the dissolved ferrous ions. Though the generated Cr(III) can be subsequently adsorbed on the FeS surface, its efficiency is dependent on the solution pH and the surface charge. Recently, organic ligands such as citrate, tartrate and oxalate are involved in promoting the Cr(VI) reduction efficiency by iron sulfide. For example, Kantar et al. found that the ligand could not only promote the FeS_2 oxidative layer dissolution to provide more active site for Cr(VI) adsorption/reduction, but also favor to the formation of Fe-Cr-ligand complexes to inhibit the mobility of Cr(VI) [30]. However, these iron sulfides are hardly separated from the reaction solution due to its limited magnetism [31]. Also, the Cr(VI) reduction/adsorption contribution with iron sulfides remains unclear in these reports.

Greigite is the thiospinel of iron that has a similar spinel crystal structure ($Fe^{2+}Fe_2^{3+}S_4$) to magnetite [32]. It is usually an authigenic ferromagnetic mineral that forms as a metastable precursor of pyrite in anoxic sedimentary environments during early diagenetic sedimentary sulfate reduction [33,34]. Due to its ferromagnetic and reductive properties, Fe_3S_4 has been widely used as material for ion batteries designing, carbon dioxide reduction and pollutants remediation [35–38]. Our previous study demonstrated that the structural sulfide of Fe_3S_4 enhanced the organoarsenic adsorption and reduction, and its reductive and adsorptive capabilities were extremely dependent on the solution pH [39]. However, there is a paucity of data concerning with the Fe_3S_4-induced Cr(VI) removal, which may be significant for the heavy metal transformation by natural iron sulfide in sediment or groundwater.

In this study, we demonstrated that the magnetic Fe_3S_4 could efficiently remove the Cr(VI). A series of experiments were designed and carried out to evaluate the effects of Cr(VI) concentration, solution pH on Cr(VI) removal efficiency. A series of approaches, such as 1,5-diphenylcarbazide coloration method, flame atomic absorption spectrometer and X-ray photoelectron spectroscopy, were used to analyze the Cr species and its adsorption/reduction contribution in the solution and on the Fe_3S_4 surface, respectively. The iron species cycle and its effects on the Cr(VI) reduction were rigorously investigated using the 1,10-phenanthrolin inhibitory experiments. This study aims to supplement the fundamentals for the adsorptive and reductive impact induced by magnetic Fe_3S_4 on Cr(VI) removal under real-world water environment.

2. Material and methods

2.1. Chemicals

Analytical grade Iron(III) nitrate nonahydrate ($Fe(NO_3)_3{\cdot}9H_2O$), thiourea, ethylene glycol (EG), ethanol, potassium dichromate ($K_2Cr_2O_7$), nitrate acid (HNO_3), 1,5-diphenylcarbazide, acetone, sulfuric acid (H_2SO_4), 1,10-phenanthrolin (Phen), sublimed sulfur, and sodium sulfide nonahydrate ($Na_2S{\cdot}9H_2O$) were purchased from Sinopharm Chemical Reagent Co. Ltd. (Shanghai, China). Suwannee River fulvic acid (SRFA-terrestrial origin) and Pony Lake fulvic acid (PLFA-microbial origin) were obtained from the International Humic Substance Society (Denver, CO, USA). All chemicals were used as received without further purification. Deionized water (> 18 MΩ·cm) was prepared by a Millipore Milli-Q system (Bedford, MA, USA) and used for all experiments.

2.2. Sample preparation

Fe_3S_4 was synthesized using a modified solvothermal method according to previous report [40]. Briefly, 1.21 g $Fe(NO_3)_3{\cdot}9H_2O$ and 0.46 g thiourea were dissolved in 60 mL of EG, and stirred at room temperature for 20 min to form a yellowish-brown solution. The resulting mixture was then transferred into a 100 mL Teflon-lined stainless steel autoclave and heated at 180 °C for 12 h. Following completion of the heating step, the autoclave was cooled to room temperature. Finally, the dark solid product was obtained by centrifugation and sequentially rinsing with distilled water and ethanol before drying in a vacuum oven at 60 °C for 6 h. The crystal structure and morphology of the as-prepared Fe_3S_4 were confirmed by powder X-ray diffraction (XRD) and scanning electron microscopy (SEM) (Figs. S1 and S2).

2.3. Characterization

Powder X-ray diffraction (XRD) patterns were acquired using a Bruker D8 Advance X-ray diffractometer with Cu Kα radiation (λ = 0.15418 nm). Scanning electron microscopy (SEM) was performed on a LEO 1450VP scanning electron microscope (Zeiss, Oberkochen, Germany). The zeta potentials of Fe_3S_4 suspensions at different pH

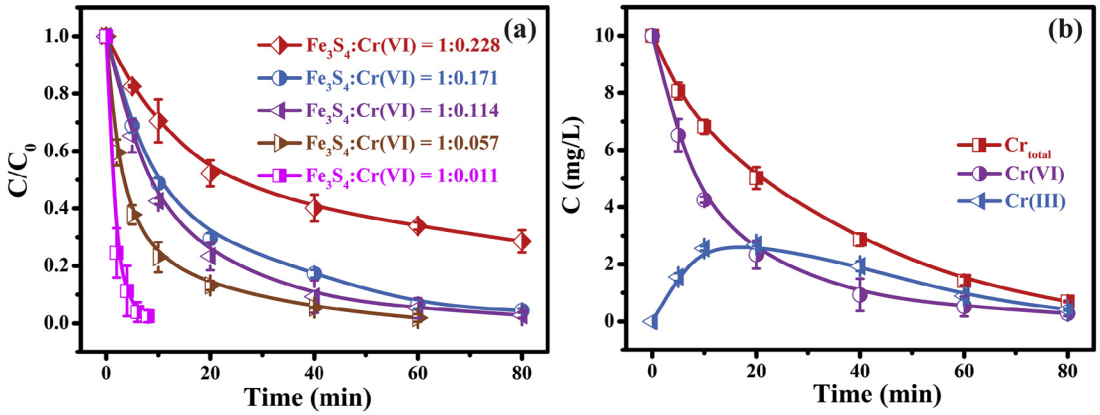

Fig. 1. (a) Effects of initial Fe_3S_4:Cr(VI) molar ratio on removal efficiency of Cr(VI) by Fe_3S_4; (b) Changes in Cr_{total}, Cr(VI) and Cr(III) concentrations at fortification level of 10 mg/L (0.192 mmol/L) of Cr(VI). The concentration of Fe_3S_4 was 0.5 g/L (1.689 mmol/L), and the initial solution pH was 5.7.

values were determined by a Malvern ZEN3690 Zetasizer (Malvern, UK). The magnetic properties of the as-prepared Fe_3S powder were determined using a vibrating sample magnetometer (VSM-7300, Quantum Design, San Diego, CA, USA) at 298 K. High-resolution X-ray photoelectron spectroscopy (XPS) was recorded with a Kratos ASIS-HS X-ray photoelectron spectroscope equipped with a standard and monochromatic source (AlKR) operated at 150 W (15 kV, 10 mA). The binding energies obtained in the XPS analysis were corrected for specimen charging by referencing the C 1s line to 284.5 eV.

2.4. Experimental procedures

The stock solution of Cr (VI) (1000 mg/L) was prepared by dissolving an appropriate dosage of $K_2Cr_2O_7$ in 100 mL deionized water and subsequently stored in the dark to avoid photochemical reaction. The working solution of Cr(VI) was prepared by an appropriate dilution of the Cr(VI) stock solution with deionized water. Cr(VI) removal experiments were carried out in 50 mL conical flasks under ambient conditions. During a typical Cr(VI) removal process, 0.01 g of Fe_3S_4 powders was added into the conical flask with 20 mL Cr(VI) solution. The flask was then covered with aluminum foil and shaken in a rotary shaker (THZ-92A, Boxun, China) at 30 °C. To explore solution pH effects, the initial pH of Cr(VI) solution was adjusted by 0.1 mol/L HCl or NaOH, and the final pH values were measured with a Sartorius basic pH meter PB-10. Anoxic Cr(VI) removal experiments were conducted in a 100 mL flask, which was vacuumed and filled with argon gas. The Cr (VI) solution was purged with argon gas for about 30 min to remove the dissolved oxygen. An 20 mg/L of SRFA or PLFA were used to clarify the effects of natural organic matters on the Cr(VI) removal by Fe_3S_4. Samples were withdrawn at a regular time interval from the flask with a syringe and passed through a 0.22 μm polytetrafluoroethylene membrane filter. To assess the stability of Fe_3S_4, the solid after reaction was separated from the solution with an additional magnet, then washed with deionized water and ethanol thoroughly, and finally vacuum-dried for the reuse. For the reactivation, the reacted Fe_3S_4 was immerged in 1 mol/L HNO_3 solution for 5 min and then washed three times with deionized water to removal the surface precipitation. All removal experiments were performed at least in triplicate.

2.5. Analytical methods

The concentration of Cr(VI) in aqueous solution was measured by using 1,5-diphenylcarbazide method [41], which was not sensitive to Cr (III) species. Chromium reagent, 1,5-diphenylcarbazide, was mixed with 0.5 mL of filtrate for 5 min. The absorbance of generated Cr(VI)-diphenylcarbazide product was determined by using a UV–Vis spectrometer (UV-752 N, INESA, China) at a wavelength of 540 nm. Total chromium (Cr(VI) and Cr(III), Cr_{total}) concentration in aqueous solution was measured with a flame atomic absorption spectrometer (Flame-AAS, PinAAcle 900T, PerkinElmer, USA). Cr(III) concentrations were calculated according to the difference between the Cr_{total} and Cr(VI) concentrations. Dissolved Fe(II) was quantified by the 1,10-phenanthrolin method [42], and total dissolved iron was obtained after adding hydroxylamine hydrochloride to the filtered solution, Fe(III) concentration was calculated by the total dissolved iron and Fe(II) concentrations. Samples were analyzed with a UV–Vis Spectrophotometer at a specific wavelength of 510 nm. Elemental sulfur in the solution was detected by a Chromaster Infinity HPLC system (Hitachi, Japan), and that adsorbed onto the Fe_3S_4 surface was extracted with ethanol prior to detection [43].

3. Results and discussions

3.1. Effects of initial Fe_3S_4:Cr(VI) molar ratio on Cr(VI) removal kinetics

The as-synthesized Fe_3S_4 was used for the removal of Cr(VI) with initial Fe_3S_4:Cr(VI) molar ratio of 1:0.011 to 1:0.228 at pH 5.7. As shown in Fig. 1a, all of the Cr(VI) concentrations decreased with prolonging reaction time from 0 to 80 min. The Cr(VI) removal efficiency almost reached as high as 100% when the initial Fe_3S_4:Cr(VI) molar ratio ranged from 1:0.011 to 1:0.171, while it decreased to 72% with the Fe_3S_4:Cr(VI) molar ratio up to 1:0.228. All of the Cr(VI) removal processes at different initial Fe_3S_4:Cr(VI) molar ratio were found to follow a pseudo-first-order kinetic equation with high correlation coefficients (Table S1). The apparent Cr(VI) removal constants decreased from 0.463 ± 0.044 to 0.015 ± 0.002 min^{-1} with increasing the initial Fe_3S_4:Cr(VI) molar ratio from 1:0.011 to 1:0.228. These observations strongly suggest that the magnetic Fe_3S_4 has a good concentration-dependent removal efficiency for Cr(VI).

3.2. Effects of natural organic matters and oxygen on Cr(VI) removal kinetics

As natural organic matters and Fe_3S_4 may co-exist in natural aquatic environments and subsequently interact with both Cr(VI) and Fe_3S_4, two kinds of NOMs (PLFA and SRFA) were evaluated for their effects on the removal efficiency of Cr(VI) by Fe_3S_4. Fig. S3 shows that Cr(VI) removal efficiencies reached up to 97% in the presence of PLFA or SRFA, indicating no significant effects of these NOMs on Cr(VI) removal. Furthermore, the effects of oxygen on the Cr(VI) removal by Fe_3S_4 was also investigated. Fig. S4 reveals that the Cr(VI) removal efficiency under argon was in general agreement with that under air conditions, ruling out the potential promotive effects of O_2 on the Fe_3S_4 oxidation and subsequent Cr(VI) removal.

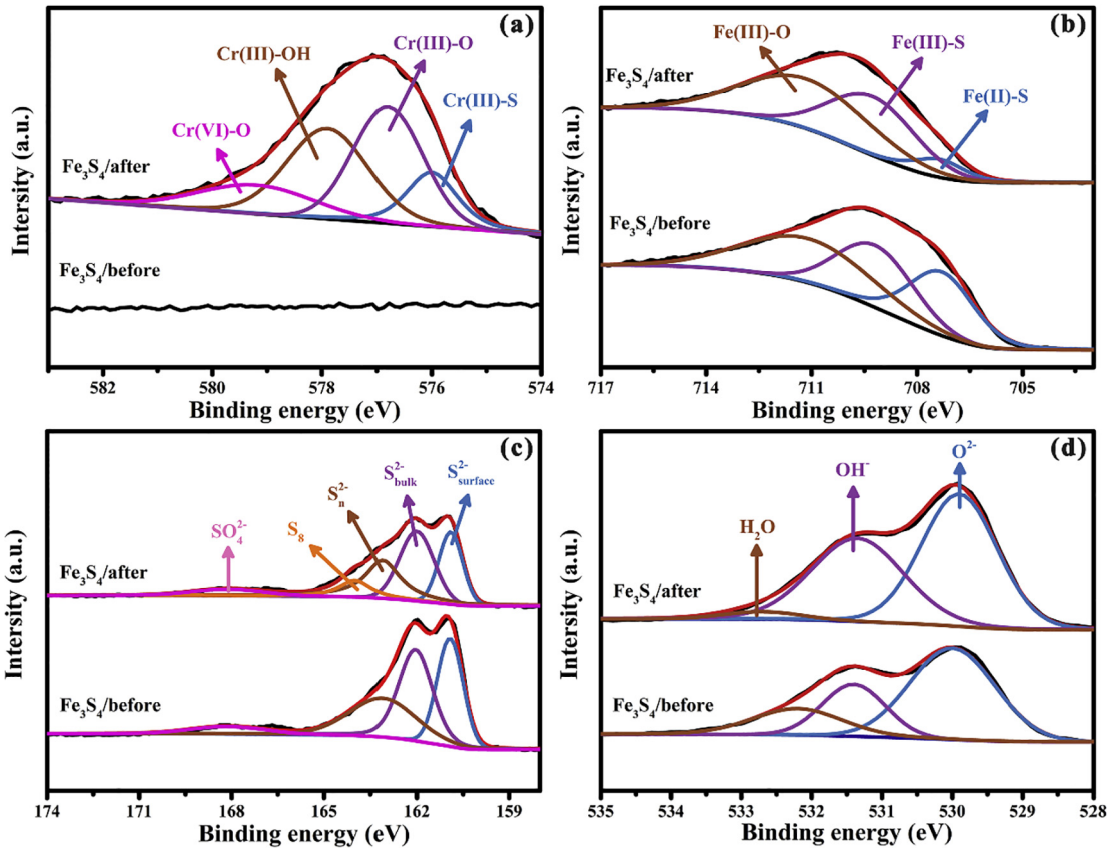

Fig. 2. High resolution XPS spectra of Fe_3S_4 before and after Cr(VI) removal. (a) Cr 2p; (b) Fe 2p; (c) S 2p and (d) O 1s, respectively. The concentrations of Fe_3S_4 and Cr(VI) were 0.5 g/L and 10 mg/L, respectively. The initial solution pH was 5.7.

3.3. Cr(VI) removal route with Fe_3S_4

Cr(VI) removal mediated with heterogeneous materials involved direct solution reduction/precipitation and surface adsorption/reduction process. Thus, the dissolved Cr(VI) and Cr_{total} concentrations during the removal process were first quantified. The Cr_{total} concentration in the solution decreased from 10.0 to 0.7 mg/L within 80 min (Fig. 1b), demonstrating that most of dissolved Cr species transferred to the Fe_3S_4 surface. Additionally, the Cr_{total} concentration was higher than that of Cr(VI), and the difference was ascribed to the generation of dissolved Cr(III). It can be found that Cr(III) concentration increased to 2.7 mg/L within 20 min, confirming the reduction of Cr(VI) with Fe_3S_4. However, the Cr(III) was then gradually decreased to 0.4 mg/L in the final 60 min, suggesting the subsequent Cr(III) adsorption/precipitation on the Fe_3S_4.

To confirm the surface adsorption and reduction of Cr(VI)/Cr(III), the Cr species on the Fe_3S_4 surface before and after the treatment were analyzed by XPS. Learning from Fig. 2a, the strong peak centered at 577.0 eV was assigned to the Cr($2p_{3/2}$) after the Cr(VI) treatment process, suggesting the generation of insoluble Cr species on the Fe_3S_4 surface. The high binding energy tail could be fitted with four peaks at 579.2, 577.9, 576.8 and 576.0 eV. The peak at 579.2 eV was attributed to the Cr(VI)-O of the $Cr_2O_7^{2-}$, and other three peaks were assigned to the Cr(III)-OH, Cr(III)-O, and Cr(III)-S of $Cr(OH)_3$, Cr_2O_3, and Cr_2S_3, respectively [44]. These results revealed that both of the Cr(VI) adsorption and reduction mechanisms were involved on the Fe_3S_4 surface. However, the relative fraction (14.8%) of Cr(VI) was much lower than that (85.2%) of Cr(III) (Table S2), suggesting the significant Cr(VI) reduction after the adsorption process with Fe_3S_4. Moreover, the high-resolution spectra of Fe 2p, S 2p and O 1s before and after Cr(VI) removal were also analyzed. The peak at 710.0 eV could be fitted at 711.1, 709.2, 707.3 eV (Fig. 2b), which were attributed to the surface Fe(III)-O, Fe(III)-S, Fe(II)-S, respectively [45]. The relative fraction of Fe(II) decreased from 30.2 to 8.6% (Table S2), which might result from the high reductive ability of Fe(II) for Cr(VI) removal. A new peak at 164.0 eV assigning to the S_8 was generated after Cr(VI) treatment, revealing the oxidation of S(-II) [46]. After that, the relative fractions of O 1s, corresponded to the oxide (529.9 eV) and hydroxide (531.4 eV), increased from 52.5% and 39.0% to 54.6% and 52.4% (Table S2), indicating the generation of Cr oxides or hydroxides [44]. Based on the above analyses, we concluded that Cr(VI) could be adsorbed on the Fe_3S_4 and reduced to Cr(III), corresponding to the Fe(II) and S(-II) oxidation.

3.4. Effects of solution pH on the Cr(VI) removal mechanism

Due to the pH-dependent reductive and adsorptive ability of Fe_3S_4, we subsequently investigated the aqueous Cr(VI) and Cr_{total} removal at pH of 3.5–10.0. It can be seen from Fig. S5 that both of Cr(VI) and Cr_{total} removal processes were extremely dependent on the initial solution pH, and all of the Cr_{total} removal efficiencies were lower than that of Cr(VI), confirming the generation of Cr(III) as described in Fig. 1b. Furthermore, the Cr_{total} and Cr(VI) removal processes were fitted well with pseudo-first-order kinetic equation with high correlation coefficients (Table 1). The apparent Cr(VI) removal rate constants ($k_{Cr(VI)}$) decreased from 0.061 to 0.017 min^{-1} with increases in solution pH from 3.5 to 10.0. However, the Cr_{total} removal rate constants ($k_{Crtotal}$) increased from 0.020 to 0.035 min^{-1} with increases in solution pH from 3.5 to 4.2, and then decreased to 0.009 min^{-1} when the solution pH reached up to 10.0. The lower pH was not only favorable to the Cr(VI) reduction due to its higher reduction ability [39], but also promote the direct electrostatic attraction when it was lower than the zeta potential (7.0) of Fe_3S_4 (Fig. S6). However, the higher pH could dramatically enhance the formation of Fe-Cr hydroxides (K_{sp},

Table 1
Pseudo-first-order rate constants of Cr(VI) ($k_{Cr(VI)}$) and Cr_{total} ($k_{Crtotal}$) by Fe_3S_4 at pH of 3.5–10.0. The concentrations of Fe_3S_4 and Cr(VI) were 0.5 g/L and 10 mg/L, respectively.

pH	Cr(VI)		Cr_{total}	
	k_{obs} (min^{-1})	R^2	k_{obs} (min^{-1})	R^2
3.5	0.061 ± 0.004	0.991	0.020 ± 0.002	0.977
4.2	0.057 ± 0.001	0.998	0.035 ± 0.001	0.997
5.7	0.043 ± 0.004	0.984	0.032 ± 0.001	0.999
7.0	0.024 ± 0.002	0.988	0.020 ± 0.001	0.995
8.5	0.023 ± 0.002	0.984	0.017 ± 0.001	0.994
10.0	0.017 ± 0.002	0.971	0.009 ± 0.001	0.963

$4 \times 10^{-38} \sim 6.3 \times 10^{-34}$ M^4) [47]. All of these contributions lead to the different tendencies of the Cr(VI) and Cr_{total} removal at pH of 3.5–10.0.

As Cr(VI) reduction and precipitation processes were accompanied by the consumption of hydrogen and hydroxyl ions, we therefore monitored the pH variations during the Cr(VI) removal processes at pH 3.5–10.0. When the initial pH was 3.5 and 4.2, the solution pH slightly increased to 4.3 and 5.0, respectively. In contrast, when the initial pH was 5.7, 7.0, 8.5 and 10.0, the solution pH slightly decreased to 5.4, 6.1, 6.4 and 7.1, respectively (Fig. S7). Because the distribution of Cr species was extremely dependent on the solution pH, Visual MINTEQ software was subsequently used to simulate the Cr species distribution curves at pH 3.0–10.0. As shown in Fig. S8, the major Cr(VI) states in aqueous solution were $HCrO_4^-$ at acidic condition, while CrO_4^{2-} at alkaline condition (Fig. S8), demonstrating occurrence of reduction and adsorption processes between $HCrO_4^-$/ CrO_4^{2-} and Fe_3S_4. In comparison, Cr(III) tended to exist as Cr(III)-hydroxylation complexes, ($Cr(OH)_2^+$, $Cr(OH)_3$ and $Cr(OH)_4^-$), at pH higher than 5.0, suggesting the potential precipitation of Cr(III) at cirumneutral or alkaline conditions. After that, the total dissolved Fe generated via the dissolution at initial pH of 3.5–10.0 was also monitored to clarify the pH effects on Fe_3S_4 dissolution. It was obvious in Fig. S9 that higher concentration of total dissolved Fe was observed at low pH, revealing the favorable dissolution of Fe_3S_4 under acidic condition. These generated Fe could subsequently promote Cr(VI) reduction and Cr(III) precipitation.

To further understand the contribution of adsorption, reduction and precipitation during the Cr(VI) removal process, the XPS was then used to analyze the surface Cr composition of the reacted Fe_3S_4 at pH of 3.5–10.0. The relative fractions of Cr(VI)-O assigned to $Cr_2O_7^{2-}$ increased from 10.8 to 26.2% over the initial pH range of 3.5–10.0 (Fig. S10 and Table 2), suggesting that the higher pH led to the higher surface Cr(VI) adsorption contribution. However, the highest Cr(III)-S, Cr(III)-O, and Cr(III)-OH relative fractions were acquired at pH 5.7, 3.5 and 10.0, respectively. These results confirmed that the solution pH could affect not only the Cr(VI) removal efficiency, but also the distribution of Cr species on the Fe_3S_4 surface. Then, we calculated the Cr(VI) and Cr(III) relative fractions to clarify the corresponding Cr(VI) adsorption and reduction/precipitation efficiencies on Fe_3S_4 surface during Cr(VI) removal process. As generalized in Table S3, the Cr(III) relative fraction decreased from 89.2 to 73.8%, corresponding to the increased Cr(VI) relative fraction from 10.8 to 26.2%, respectively. The higher fraction of Cr(III) relative to Cr(VI) at pH of 3.5–10.0 confirmed the dominant contribution of Cr(VI) reduction and subsequent Cr(III) precipitation during the Cr(VI) removal process.

3.5. Cr(VI) reduction mechanism

As Cr(VI) may be reduced by ferrous ions or sulfide-species released via the redox of Fe_3S_4, it is necessary to clarify the effects and contributions of reactive reductant on Cr(VI) removal process. 1,10-Phenanthroline was first employed to complex both the surface and dissolved Fe(II) to inhibit their effects on Cr(VI) reduction [48]. Because the maximum absorption spectrum (510 nm) of $Fe(phen)_3^{2+}$ had partial overlapping of Cr(VI) detection via 1,5-diphenylcarbazide method (540 nm), Cr_{total} was used to evaluate the effects of 1,10-phenanthroline on the Cr(VI) removal. The Cr_{total} removal efficiency was sharply suppressed by 1,10-phenanthroline (Fig. 3a), and Cr_{total} pseudo-first-order removal rate constants decreased from 0.032 to 0.011 min^{-1} (the inset of Fig. 3a). The inhibitory efficiency (η) of 1,10-phenanthroline in the Cr_{total} removal with Fe_3S_4 was computed by the following equation (1) [49].

$$\eta\% = \left[\frac{k_0 - k_1}{k_0}\right] \times 100\% \quad (1)$$

where k_0 and k_t are the apparent Cr_{total} removal rate constants in the absence and the presence of 1,10-phenanthroline, respectively. The inhibitory efficiency reached as high as 65.6%, which was ascribed to the inhibition of Fe(II)-mediated Cr(VI) reduction and subsequently Cr(III) adsorption/precipitation process. This high percentage confirmed the dominated contribution of Fe(II) rather than S(II) on the Cr(VI) reduction by Fe_3S_4.

To prove the specific reaction between Fe(II) and Cr(VI), the iron species released by the redox of Fe_3S_4 with/without Cr(VI) were systematically investigated. Fig. 3b shows that the Fe(II) concentrations were sharply increased to 11.0 mg/L within 20 min and then gradually increased to 12.3 mg/L at 80 min without Cr(VI). However, it was only 0.8 mg/L at 20 min and subsequently decreased to 0.7 mg/L within 80 min in the presence of Cr(VI). The lower ferrous ions obtained in the presence of Cr(VI) confirmed the direct reaction between Fe(II) and Cr(VI). Moreover, the ferric ions in the two systems were extremely lower than ferrous ions, which might result from the formation of iron-hydroxylation complexes (K_{sp}, $Fe(OH)_3$, 4×10^{-38} M^4) and subsequently adsorption on the Fe_3S_4 surface at pH 5.7. The final Fe(III) concentration (0.5 mg/L) in the presence of Cr(VI) was higher than that (0.2 mg/L) in the absence of Cr(VI), suggesting more generation of Fe(III) via the redox reaction between Fe(II) and Cr(VI). These generated Fe(III) could hardly react with Cr(VI) and inhibit the Cr(VI) removal efficiency by prolonging the reaction time. Over the initial concentration range of 1.0 ~ 20.0 mg/L, the stable apparent removal constants of Cr(VI) suggested occurrence of the continual reaction between ferrous ions and Cr(VI) (Table S1). Therefore, it is necessary to further investigate the transformation mechanisms on iron species during the Cr(VI) removal process.

Our previous studies confirmed that FeS_2 induced the oxygen

Table 2
XPS results based on curve fitting for Cr $2p_{3/2}$ peaks of Fe_3S_4 before and after the Cr(VI) removal at pH of 3.5–10.0. The concentrations of Fe_3S_4 and Cr(VI) were 0.5 g/L and 10 mg/L, respectively.

B. E. (eV)	Species	Relative fraction (%)					
		pH = 3.5	pH = 4.2	pH = 5.7	pH = 7.0	pH = 8.5	pH = 10.0
576.0	Cr(III)-S	7.7	14.2	14.9	15.5	12.1	10.5
576.8	Cr(III)-O	52.6	40.7	35.9	29.2	26.2	21.2
577.9	Cr(III)-OH	28.9	32.9	34.4	38.7	41.4	42.1
579.2	Cr(VI)-O	10.8	12.2	14.8	16.6	20.3	26.2

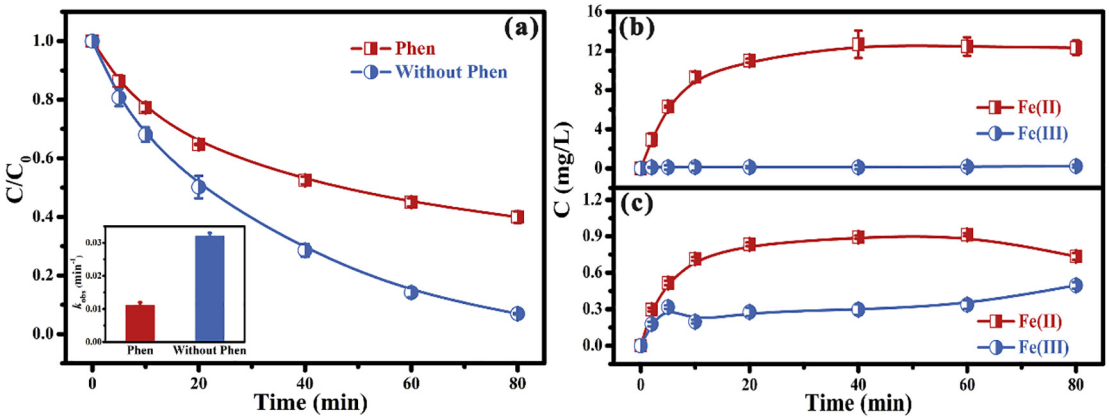

Fig. 3. (a) Cr_{total} removal efficiency with Fe_3S_4 in the absence and presence of 1,10-phenanthrolin; the inset shows the Cr_{total} pseudo-first-order removal rate constants; (b) and (c) time profile of dissolved Fe(II) and Fe(III) released from Fe_3S_4 in the absence and presence of Cr(VI). The concentrations of Fe_3S_4, Cr(VI) and 1,10-phenanthrolin were 0.5 g/L, 10 mg/L and 5 g/L, respectively. The initial solution pH was 5.7.

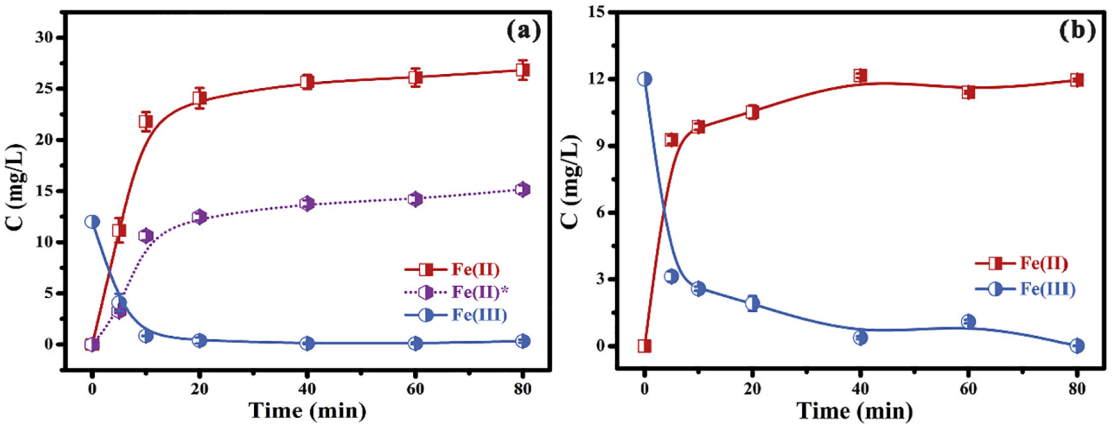

Fig. 4. Time profiles of Fe(III) and Fe(II) in the (a) Fe(III)/Fe_3S_4/H_2O system; (b) Fe(III)/S(-II) system. The additional Fe(III) and S(-II) concentrations were 12 mg/L and 216 mg/L, respectively. The concentration of Fe_3S_4 was 0.5 g/L, and the initial solution pH was 5.7.

activation to generate supper oxygen anions via a single electron transformation mechanism by the surface ferrous ions to promote the surface Fe(III)/Fe(II) [42]. Thus, we subsequently verified the potential Fe(III)/Fe(II) cycles during the Cr(VI) removal process with Fe_3S_4. Upon addition of Fe(III) (12.0 mg/L), Fig. 4a shows the changing trend between Fe(III) and Fe(II) concentrations in the Fe_3S_4/H_2O system. Obviously, the Fe(III) concentration sharply decreased from 12.0 to 0.4 and 0.3 mg/L within 20 and 80 min, respectively. Correspondingly, the Fe(II) increased from 0 to 24.1 and 26.8 mg/L within 20 and 80 min, suggesting the rapid Fe(III) reduction and Fe(II) generation induced by Fe_3S_4. Because the Fe(II) could be released by the redox/dissolution of Fe_3S_4 and the reduction of the additional Fe(III) in the Fe(III)/Fe_3S_4/H_2O system, the actual Fe(II) concentration generated via the dissolution/redox of Fe_3S_4 was calculated according to the difference between the total Fe(II) generation and the Fe(II) corresponding to the Fe(III) reduction in the Fe(III)/Fe_3S_4/H_2O system. Learning from Fig. 3b, the final Fe(II) concentration ($Fe(II)^*$, 15.2 mg/L) generated via the dissolution/redox of Fe_3S_4 was slightly higher than that (12.3 mg/L) in the Fe_3S_4/H_2O system (Fig. 3b), which might result from the enhanced dissolution/redox of Fe_3S_4 in the presence of additional Fe(III). Due to the presence of both Fe and S in Fe_3S_4, we thus inferred that the electron-donator for the Fe(III) reduction might result from the sulfides. In the presence of sulfide ions (Fe(III)/S(-II) system), the Fe(III) sharply decreased to 2.0 mg/L within 20 min and gradually decreased to 0.01 mg/L from 20 to 80 min (Fig. 4b). Correspondingly, the Fe(II) gradually increased to 10.5 mg/L within 20 min and remained nearly constant at 12.0 mg/L in the final 60 min. These observations indicated that the generated Fe(III) during the Cr(VI) removal process could be reduced by sulfides of Fe_3S_4.

Corresponding to the Fe(III) reduction, the probable oxidation products of sulfide was monitored during the Cr(VI) removal with Fe_3S_4. Similar as our previous study [39], limited dissolved sulfate or sulfite ions were detected during the redox of Cr(VI) with Fe_3S_4. Then, the elemental sulfur concentration was monitored in the solution and on the Fe_3S_4 surface. It can be seen from Fig. S11 that the dissolved elemental sulfur was extremely low, and that the surface elemental sulfur gradually increased to 1.3 mg/L within 20 min, possibly due to its strong hydrophobicity and limited solubility. Subsequently, the effects of sulfur-byproducts, such as elemental sulfur and sulfide ions, on the Cr(VI) reduction were investigated. As shown in Fig. S12, Cr(VI) was negligibly reduced by the elemental sulfur in the solution, ruling out the direct Cr(VI) reduction and/or adsorption by elemental sulfur. It was worth mentioning that only 25% of Cr(VI) could be reduced in the presence of dissolved sulfide ions, confirming the limited contribution of sulfide on the Cr(VI) reduction. Therefore, it could be concluded that the sulfide originating from the Fe_3S_4 surface promoted the surface Fe (III)/Fe(II) cycles rather than the direct Cr(VI) reduction, which was consistent with the observations of 1,10-phenanthroline inhibitory experiments (Fig. 3a).

According to the above findings, we proposed a possible Cr(VI) adsorption and reduction mechanism by magnetic Fe_3S_4 (Scheme 1). Under weak acid condition, Cr(VI) is adsorbed on the surface of Fe_3S_4 via the electrostatic attraction and reduced by the surface ferrous to generated Cr(III). Meanwhile, Fe_3S_4 is oxidized to release dissolved

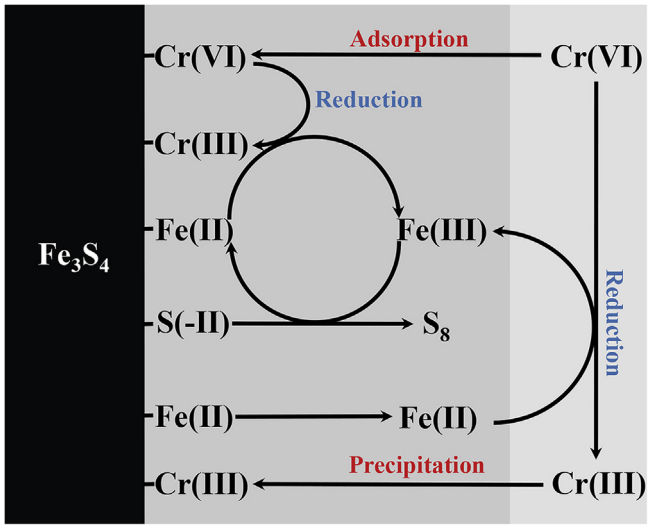

Scheme 1. Proposed Cr(VI) removal mechanism with magnetic Fe_3S_4.

ferrous ions and sulfides, and the dissolved ferrous ions promote the aqueous Cr(VI) reduction. The dissolved Cr(III) could be subsequently transformed as Cr (oxide)hydroxyl and sulfide to realize the stability of Cr species. Otherwise, the generated Fe(III) can be reduced to Fe(II) by the sulfide, corresponding to the generation of elemental sulfur. These transformation of Fe(III)/Fe(II) occurs on the Fe_3S_4 surface, which increases the Cr(VI) removal efficiency. Under weak alkaline condition, the electrostatic attraction between Cr(VI) and Fe_3S_4 was blocked by the negatively charged Fe_3S_4 surface. Furthermore, the reductive ability of Fe_3S_4 was also decreased at higher pH. Both of these effects lead to the lower Cr(VI) removal by Fe_3S_4 at higher pH.

3.6. *Reusability of Fe_3S_4 for Cr(VI) removal*

The stability of reactant is a key issue for their practical application. Therefore, the used magnetic Fe_3S_4 was separated from the suspension and reused for the Cr(VI) removal under the same conditions. The Fe_3S_4 appeared excellent magnetism after three cycles (Fig. S13); however, its total Cr(VI) removal efficiency decreased from 97% to 41% and 37% at 2nd and 3rd cycles (Fig. S14), respectively. The gradual decrease in Cr (VI) removal efficiency with Fe_3S_4 might attribute to the surface inactivation, which was reflected in that the iron(chromium)-hydroxylation peaks were observed in the XPS (Fig. 2). To reactivate Fe_3S_4, the Cr (VI)-reacted Fe_3S_4 was treated by dilute HNO_3 solution to dissolve the surface iron(chromium)-hydroxylation, and reused for the 4th cycle. As shown in Fig. S14, the Cr(VI) removal increased up to 65.8% after the reactivation of Fe_3S_4. The difference in the removal efficiencies between 1st and 4th cycles could be attributed to difficult and incomplete activation of the Fe_3S_4 surface by a simple picking process.

4. Conclusions

In summary, the present study employed magnetic Fe_3S_4 as a novel and effective material for Cr(VI) removal. The total Cr(VI) removal process was involved in the surface adsorption, surface reduction and solution reduction at pH 3.5–10.0, resulting in the immobilization of Cr_2O_3, $Cr(OH)_3$, and Cr_2S_3 on the Fe_3S_4 surface, and the highest surface reaction efficiency was obtained at pH 7.0. Moreover, the high Cr(VI) removal efficiency by the Fe_3S_4 was highly dependent on the structural sulfides, which supplied electrons to Fe(III) rather than Cr(VI) and thus promote the Fe(III)/Fe(II) cycles. The easy separation by additional magnet makes the low-cost iron sulfides to be a potential material for heavy metal removal in contaminated waters.

Acknowledgements

This work was jointly supported by National Science Foundation (Grants 21577107, 21707105 and 21876125), Zhejiang Provincial Public Benefit Project (Grant LGF18B070004 and LGF19B070009), Wenzhou City Water Pollution Control and Governance Technology Innovation Project (Grant W20170017), Zhejiang Provincial Xinmiao Talent Project (Grant 2017R413033), and the Research and Development Fund of Wenzhou Medical University (Grant QTJ16013).

Appendix A. Supplementary data

Supplementary data to this article can be found online at https://doi.org/10.1016/j.cej.2018.11.192.

References.

[1] J. Gorny, G. Billon, C. Noiriel, D. Dumoulin, L. Lesven, B. Madé, Chromium behavior in aquatic environments: a review, Environ. Rev. 24 (2017) 503–516.
[2] J. Kotaś, Z. Stasicka, Chromium occurrence in the environment and methods of its speciation, Environ. Pollut. 107 (2000) 263–283.
[3] D.E. Kimbrough, Y. Cohen, A.M. Winer, L. Creelman, C. Mabuni, A critical assessment of chromium in the environment, Crit. Rev. Environ. Sci. Technol. 29 (1999) 1–46.
[4] A.D. Bokare, W. Choi, Advanced oxidation process based on the Cr(III)/Cr(VI) redox cycle, Environ. Sci. Technol. 45 (2011) 9332–9338.
[5] T. Xu, K. Patel, J.R. Ridpath, J.A. Swenberg, J. Nakamura, Genotoxicity of trace level of hexavalent chromium existing in city water, Cancer Res. 74 (2014) 5363.
[6] S.A. Katz, H. Salem, The toxicology of chromium with respect to its chemical speciation: a review, J. Appl. Toxicol. 13 (1993) 217–224.
[7] H. Lyu, J. Tang, Y. Huang, L. Gai, E.Y. Zeng, K. Liber, Y. Gong, Removal of hexavalent chromium from aqueous solutions by a novel biochar supported nanoscale iron sulfide composite, Chem. Eng. J. 322 (2017) 516–524.
[8] S. Loyaux-Lawniczak, P. Lecomte, J.J. Ehrhardt, Behavior of hexavalent chromium in a polluted groundwater: redox processes and immobilization in soils, Environ. Sci. Technol. 35 (2001) 1350–1357.
[9] H. Chang, J.H. Singer, J.C. Seaman, In situ chromium(VI) reduction using iron(II) solutions: modeling dynamic geochemical gradients, Vadose Zone J. 11 (2012) 1043–1053.
[10] B. Deng, L. Lan, K. Houston, P.V. Brady, Effects of clay minerals on Cr(VI) reduction by organic compounds, Environ. Monit. Assess. 84 (2003) 5–18.
[11] M. Pettine, D. Tonnina, F.J. Millero, Chromium(VI) reduction by sulphur(IV) in aqueous solutions, Mar. Chem. 99 (2015) 31–41.
[12] E.A. Kaprara, A.I. Zouboulis, K.T. Simeonidis, M.G. Mitrakas, Potential application of inorganic sulfur reductants for Cr(VI) removal at sub-ppb level, Desalin. Water Treat. 54 (2015) 2067–2074.
[13] J.C. Seaman, P.M.B. And, L. Schwallie, In situ Cr(VI) reduction within coarse-textured, oxide-coated soil and aquifer systems using Fe(II) solutions, Environ. Sci. Technol. 33 (1999) 938–944.
[14] M.A. Schlautman, I. Han, Effects of pH and dissolved oxygen on the reduction of hexavalent chromium by dissolved ferrous iron in poorly buffered aqueous systems, Water Res. 35 (2001) 1534–1546.
[15] C. Kim, Q. Zhou, B. Deng, E.C. Thornton, H. Xu, Chromium(VI) reduction by hydrogen sulfide in aqueous media: stoichiometry and kinetics, Environ. Sci. Technol. 35 (2001) 2219–2225.
[16] Q. Liu, M. Xu, F. Li, T. Wu, Y. Li, Rapid and effective removal of Cr(VI) from aqueous solutions using the $FeCl_3$/$NaBH_4$ system, Chem. Eng. J. 296 (2016) 340–348.
[17] M. Villacís-García, M. Villalobos, M. Gutiérrez-Ruiz, Optimizing the use of natural and synthetic magnetites with very small amounts of coarse Fe(0) particles for reduction of aqueous Cr(VI), J. Hazard. Mater. 281 (2015) 77–86.
[18] Y. Zou, X. Wang, A. Khan, P. Wang, Y. Liu, A. Alsaedi, T. Hayat, X. Wang, Environmental remediation and application of nanoscale zero-valent iron and its composites for the removal of heavy metal ions: a review, Environ. Sci. Technol. 50 (2016) 7290–7304.
[19] F. Pinakidou, M. Katsikini, K. Simeonidis, E. Kaprara, E.C. Paloura, M. Mitrakas, Paloura, M. Mitrakas, On the passivation mechanism of Fe_3O_4 nanoparticles during Cr(VI) removal from water: a XAFS study, Appl. Surf. Sci. 360 (2016) 1080–1086.
[20] L. Di Palma, M.T. Gueye, E. Petrucci, Hexavalent chromium reduction in contaminated soil: a comparison between ferrous sulphate and nanoscale zero-valent iron, J. Hazard. Mater. 281 (2015) 70–76.
[21] J. Du, J. Bao, C. Lu, D. Werner, Reductive sequestration of chromate by hierarchical FeS@Fe^0 particles, Water Res. 102 (2016) 73–81.
[22] S. Jo, J.Y. Lee, S.H. Kong, J. Choi, J.W. Park, Iron monosulfide as a scavenger for dissolved hexavalent chromium and cadmium, Environ. Technol. 29 (2008) 975–983.
[23] Y. Mu, F. Jia, Z. Ai, L. Zhang, Iron oxide shell mediated environmental remediation properties of nano zero-valent iron, Environ. Sci.: Nano 4 (2017) 27–45.
[24] Y. Liu, W. Xiao, J. Wang, Z.A. Mirza, T. Wang, Optimized synthesis of FeS nanoparticles with a high Cr(VI) removal capability, J. Nanomater. 2016 (2016)

7817296.
[25] C. Kantar, C. Ari, S. Keskin, Z.G. Dogaroglu, A. Karadeniz, A. Alten, Cr(VI) removal from aqueous systems using pyrite as the reducing agent: Batch, spectroscopic and column experiments, J. Contam. Hydrol. 174 (2015) 28–38.
[26] Y.T. Lin, C.P. Huang, Reduction of chromium(VI) by pyrite in dilute aqueous solutions, Sep. Purif. Technol. 63 (2008) 191–199.
[27] A.M. Graham, E.J. Bouwer, Oxidative dissolution of pyrite surfaces by hexavalent chromium: surface site saturation and surface renewal, Geochim. Cosmochim. Acta 83 (2013) 379–396.
[28] F. Demoisson, M. Mullet, B. Humbert, Pyrite oxidation by hexavalent chromium: investigation of the chemical processes by monitoring of aqueous metal species, Environ. Sci. Technol. 39 (2005) 8747–8752.
[29] R.R. Patterson, S. Fendorf, M. Fendorf, Reduction of hexavalent chromium by amorphous iron sulfide, Environ. Sci. Technol. 31 (1997) 2039–2044.
[30] C. Kantar, C. Ari, S. Keskin, Comparison of different chelating agents to enhance reductive Cr(VI) removal by pyrite treatment procedure, Water Res. 76 (2015) 66–75.
[31] Y. Gong, L. Gai, J. Tang, J. Fu, Q. Wang, E.Y. Zeng, Reduction of Cr(VI) in simulated groundwater by FeS-coated iron magnetic nanoparticles, Sci. Total. Environ. 595 (2017) 743–751.
[32] D. Rickard, L.G. Rd, Chemistry of iron sulfides, Chem. Rev. 38 (2007) 514–562.
[33] I. Letard, P. Sainctavit, N. Menguy, J.P. Valet, A. Isambert, M.J. Dekkers, A. Gloter, Mineralogy of greigite Fe_3S_4, Phys. Scripta T115 (2005) 489–491.
[34] A.P. Roberts, L. Chang, C.J. Rowan, C.S. Horng, F. Florindo, Magnetic properties of sedimentary greigite (Fe_3S_4): an update, Rev. Geophys. 49 (2011) RG1002.
[35] Q. Li, Q. Wei, W. Zuo, L. Huang, W. Luo, Q. An, V.O. Pelenovich, L. Mai, Q. Zhang, Greigite Fe_3S_4 as a new anode material for high-performance sodium-ion batteries, Chem. Sci. 8 (2017) 160–164.
[36] A. Roldan, N.H. de Leeuw, Methanol formation from CO_2 catalyzed by Fe_3S_4{111}: formate versus hydrocarboxyl pathways, Faraday Discuss. 188 (2015) 161–180.
[37] L. Kong, L. Yan, Z. Qu, N. Yan, L. Li, β-Cyclodextrin stabilized magnetic Fe_3S_4 nanoparticles for efficient removal of Pb(II), J. Mater. Chem. A 3 (2015) 15755–15763.
[38] Y. Zhou, Y. Zhao, X. Wu, W. Yin, J. Hou, S. Wang, K. Feng, X. Wang, Adsorption and reduction of hexavalent chromium on magnetic greigite (Fe_3S_4)-CTAB: leading role of Fe(II) and S(−II), RSC Adv. 8 (2018) 31568–31574.
[39] W. Liu, Z. Ai, R.A. Dahlgren, L. Zhang, X. Wang, Adsorption and reduction of roxarsone on magnetic greigite (Fe_3S_4): indispensable role of structural sulfide, Chem. Eng. J. 330 (2017) 1232–1239.
[40] Z.J. Zhang, X.Y. Chen, Magnetic greigite (Fe_3S_4) nanomaterials: shape-controlled solvothermal synthesis and their calcination conversion into hematite (α-Fe_2O_3) nanomaterials, J. Alloys Compd. 488 (2009) 339–345.
[41] W. Shen, Y. Mu, T. Xiao, Z. Ai, Magnetic Fe_3O_4-FeB nanocomposites with promoted Cr(VI) removal performance, Chem. Eng. J. 285 (2016) 57–68.
[42] W. Liu, Y.Y. Wang, Z.H. Ai, L.Z. Zhang, Hydrothermal synthesis of FeS_2 as a high-efficiency fenton reagent to degrade alachlor via superoxide-mediated Fe(II)/Fe(III) cycle, ACS Appl. Mater. Inter. 7 (2015) 28534–28544.
[43] T. Gao, Y. Shi, F. Liu, Y. Zhang, X. Feng, W. Tan, G. Qiu, Oxidation process of dissolvable sulfide by synthesized todorokite in aqueous systems, J. Hazard. Mater. 290 (2015) 106–116.
[44] H. Lyu, H. Zhao, J. Tang, Y. Gong, Y. Huang, Q. Wu, B. Gao, Immobilization of hexavalent chromium in contaminated soils using biochar supported nanoscale iron sulfide composite, Chemosphere 194 (2018) 360–369.
[45] W. Han, M. Gao, Investigations on iron sulfide nanosheets prepared via a single-source precursor approach, Cryst. Growth Des. 8 (2008) 1023–1030.
[46] J. Wu, X.B. Wang, R.J. Zeng, Reactivity enhancement of iron sulfide nanoparticles stabilized by sodium alginate: taking Cr (VI) removal as an example, J. Hazard. Mater. 333 (2017) 275–284.
[47] L. Huang, C.H. Yu, P.K. Hopke, J.Y. Shin, Z. Fan, Trivalent chromium solubility and its influence on quantification of hexavalent chromium in ambient particulate matter using EPA method 6800, J. Air Waste Manage. 64 (2014) 1439–1445.
[48] H. Zhou, Y. He, Y. Lan, J. Mao, S. Chen, Influence of complex reagents on removal of chromium(VI) by zero-valent iron, Chemosphere 72 (2008) 870–874.
[49] W. Liu, Z. Ai, M. Cao, L. Zhang, Ferrous ions promoted aerobic simazine degradation with Fe@Fe_2O_3 core–shell nanowires, Appl. Catal. B: Environ. 150–151 (2014) 1–11.